The electronic structure of the calcium monohalides. A ligand field approach

Steven F. Rice, Hans Martin, and Robert W. Field

Citation: The Journal of Chemical Physics **82**, 5023 (1985); doi: 10.1063/1.448676
View online: https://doi.org/10.1063/1.448676
View Table of Contents: http://aip.scitation.org/toc/jcp/82/11
Published by the American Institute of Physics

The electronic structure of the calcium monohalides. A ligand field approach

Steven F. Rice
Department of Chemistry, Massachusetts Institute of Technology, Cambridge, Massachusetts 02139
Hans Martin
Institute of Physics, University of Stockholm, Vanadisvägen 9, S-11346 Stockholm, Sweden
Robert W. Field
Department of Chemistry, Massachusetts Institute of Technology, Cambridge, Massachusetts 02139

(Received 13 November 1984; accepted 20 February 1985)

The electronic structure of the calcium monohalides is addressed using a ligand field model which approximates the halide as a polarizable negative charge perturbing the one electron valence structure of the Ca^+ ion. A simple, zero-free-parameter model is shown to predict accurately electronic energies, transition moments, permanent dipole moments, and several other molecular constants that have been experimentally determined. The molecular properties and electronic wave functions are interpreted in terms of the polarization ($s/p/d$ /f mixing) and radial expansion ($nl/n + 1l$ mixing) of the low lying, free ion, basis functions caused by the electric field of the ligand.

INTRODUCTION

We present here a semiempirical electrostatic model for the electronic structure of the calcium monohalides. Based on the assumptions of ligand field theory, treating the ligand as a point charge and explicitly evaluating the electrostatic interactions present, this model clearly shows that most electronic properties (e.g., excited state energies, dissociation energies, permanent dipole moments, transition moments, and second order terms in the effective ($^2\Pi$, $^2\Sigma^+$) Hamiltonian arising from rotation-electronic coupling) of these CaX molecules may be derived from the experimentally observed properties of the atomic ion states and the calculated shape and size of the atomic orbitals of the free Ca^+ ion. In this treatment, a molecular Hamiltonian which approximates the halide as a polarizable point charge is introduced as a perturbation on the free ion Hamiltonian. The eigenvalues and eigenfunctions of this Hamiltonian are obtained using degenerate perturbation theory. The success of this electrostatic model in this essentially one-electron system raises the possibility of applying the simple concepts of ligand field theory to the electronic structure of more complex diatomic molecules.

The alkaline earth monohalide molecules have received a great deal of attention, partly because of their simple electronic structure as first suggested by Knight *et al.*[1] Based on this suggestion, Dagdigian *et al.*[2] devised a one-electron picture involving only Ca^+ 4*s* and 4*p* orbitals to explain the radiative lifetimes of the CaX $A\,^2\Pi$ and $B\,^2\Sigma^+$ excited states. Dagdigian *et al.* also indicated that a simple ligand field model, presumably similar to that presented here, failed to account for the experimental observations. Preceding these[1,2] experiments, Dunn[3] had discussed scandium monoxide (isoelectronic with CaF) and had suggested a qualitative interpretation of the energy levels in the spirit of ligand field theory. However, no attempt was made to calculate explicitly energy levels or other molecular properties based on a point charge model. Bernath *et al.*[4] developed a model similar to that in Ref. 2 using hyperfine splittings due to the halogen. Klynning and Martin,[5] in a different approach, applied a Rittner polarization model[6] to several states of CaCl and obtained agreement with the lifetimes reported in Ref. 2 and the spin orbit splitting present in the $A\,^2\Pi$ state. Very recently Törring *et al.*[7] have expanded on this polarization model and have obtained accurate dissociation energies and vibrational anharmonicities for all the Group IIa monohalides. In addition to these semiempirical models, *ab initio* calculations on CaF[8] and CaCl[9] have been reported.

Despite the apparent simplicity of their electronic structure, the $A\,^2\Pi$–$X\,^2\Sigma^+$ and $B\,^2\Sigma^+$–$X\,^2\Sigma^+$ transitions are observed as highly congested band systems in the optical spectrum of the alkaline earth monohalides. The availability of tunable lasers has greatly aided the analysis of these band systems. The analysis of the *A*–*X* and *B*–*X* systems is now complete for all the calcium monohalides, thus enabling precise determination of not only rotation–vibration properties[10(a)-10(f)] but rotation-electronic[10(f)-10(h)] and pure electronic properties such as hyperfine interactions,[10(h),10(i)] spin orbit coupling, and Λ doubling. In addition, the rotational analyses have made other types of experiments possible, such as radiofrequency- and microwave-optical double-resonance experiments that have provided high precision determinations of hyperfine parameters[10(j)-10(o)] and ground state permanent dipole moments.[11-14] This extensive set of experimental results for the calcium monohalides provides a variety of stringent tests of any electronic structure model.

THE MODEL

The ligand field model assumes that the valence electronic structure of these molecules can be represented by one electron in an orbital outside the M^{2+} and X^- filled shells. This electron (4*s* in the ground state of the free Ca^+ ion) is highly polarizable because of the ease of mixing with other functions such as 3*d* and 4*p* lying just a few eV to higher energy. A small admixture of these slightly higher energy orbitals allows the alkaline earth monohalide ground state to have an electron density distribution such that the negative charge in this lowest energy, singly occupied, metal-centered, valence orbital is shifted away from the X^- charge,

 0021-9606/85/115023-12$02.10

thus stabilizing the system. In this ionic description, the low lying states of MX are described by one electron outside closed shells placed in any one of a number of orbitals that are linear combinations of Ca^+ 4*s*, 4*p*, and 3*d* (and smaller amounts of 5*s*, 5*p*, 4*d*, and 4*f*).

The model rests on the assumption that the electronic states of a molecule or complex can be described as a linear combination of functions associated with a central free ion and that the other atoms in the system can be represented as point charges (or dipoles). The ligand field model has a particularly simple form when the ligand has a closed shell electronic structure. A closed shell ligand structure would introduce no additional complexity due to orbital degeneracy or low lying ligand atomic LS terms and would be less polarizable than an open shell. In the special case of a metal–halide diatomic molecule, the assumptions of the model require the molecule to be well represented by configurations corresponding to M^+X^-. Herzberg[15] has suggested a criterion for determining the extent to which the M^+X^- valence configurations are present in the ground state of a diatomic molecule. If the internuclear distance at which the ionic and covalent curves cross R_x is greater than twice the equilibrium internuclear configuration R_e then the ground state should be completely ionic. Hildenbrand[16] has shown that this is a valid criterion for many of the Group IIa monohalides and that it leads to accurate predictions for all of the CaX molecules. Based on Rittner's polarization model,[6] Hildenbrand showed that the dissociation energies of all four CaX molecules can be accounted for in terms of simple point multipole electrostatic interactions, and one term accounting for the closed shell repulsion at short internuclear distance. There is essentially no covalent bonding in this representation of the ground states in this family of molecules. The success of the Rittner approach for the alkali monohalides and for this particular property of the alkaline earth monohalides makes an ionic model appear attractive as a starting point for the interpretation and prediction of other electronic properties of the Group IIa monohalides. In addition, measurements of hyperfine coupling constants[4,8] in the calcium monohalides are consistent with the high degree of ionicity prerequisite for the application of an electrostatic ionic model such as ligand field theory.

LIGAND FIELD CALCULATION

The model used here is essentially a "crystal field" calculation in the sense that all electronic radial integrals are explicitly evaluated. However, because this gas phase molecular system is not in a crystalline environment, the term "ligand field" is used throughout to avoid confusion.

The ligand field model for the electronic structure of the alkaline earth monohalides partitions a molecule into three mutually interacting subsystems: the M^{2+} closed shell ion, the X^- closed shell ion, and the M^{2+}-centered valence electron. The ligand field Hamiltonian for the electronic states of the MX molecule is

$$H = \text{I.P.(M)} - \text{E.A.(X)} - \frac{2e^2}{R_{MX}} + |i\rangle E_i^{FI}\langle i| + H^{CF}(R_{MX}), \tag{1}$$

where I.P. and E.A. are the ionization potential and electron affinities of the neutral M and X atoms, $2e^2/R_{MX}$ is the attractive electrostatic interaction of the M^{2+} ion core with the X^- ligand treated as a point charge at the internuclear separation R_{MX}, E_i^{FI} and $|i\rangle$ are the free M^+ ion energy levels[17] and eigenfunctions with the zero of energy set at the $M^0 \rightarrow M^+ + e^-$ ionization limit, and H^{CF} represents the interaction of the valence electron on the M^{2+} center with the ligand negative charge. H^{CF} is not diagonal in the free-M^+-ion orbital basis set.

I.P.(M), E.A.(X), and E_i^{FI} are previously measured experimental values. The electrostatic attraction energy can be evaluated for any bond distance of interest. Both the real X^- and M^{2+} ions have ionic radii which reflect the spatial extent of their closed shells. At the equilibrium internuclear distance, the repulsive force from the interaction of these closed shells balances the ionic attraction described by Eq. (1). In the present approximation we assume that this repulsive interaction is independent of the orbital occupied by the valence electron. In fact, since the first three terms in Eq. (1) are independent of the valence electrons, these terms can be ignored when determining the metal ion orbital mixing and relative energy levels of the molecule, leaving only E_i^{FI} and $H^{CF}(R_{MX})$ to be included in the ligand field calculation.

In a diatomic molecule, the point charge contribution to the Hamiltonian takes the form

$$H^{CF}(R_{MX}) = \sum_{n=1}^{N} \sum_{k=0}^{\infty} C_{k0}^n B_{k0}^n(R_{MX}), \tag{2}$$

where C_{k0}^n are modified spherical harmonics of rank k for the nth electron. The summation in n is over all electrons on the metal center outside the closed shell. The B_{k0}^n's are one-electron radial operators of the form

$$B_{k0}^n = \frac{e^2 r_n^k}{R_{MX}^{k+1}}, \quad r_n < R_{MX}$$

$$= \frac{e^2 R_{MX}^k}{r_n^{k+1}}, \quad r_n > R_{MX}, \tag{3}$$

where R_{MX} is the molecular internuclear distance and r_n is the distance of the nth electron from the metal center. The infinite k summation is rigorously truncated in the evaluation of the Hamiltonian matrix elements in the M^+ valence orbital basis by triangle conditions associated with the $\int Y_{lm}(\theta,\phi) C_{k0}(\theta,\phi) Y_{l'm'}(\theta,\phi) \sin\theta \, d\theta \, d\phi$ angular integrals. The eigenvalues of $H^{CF} + |i\rangle E_i^{FI}\langle i|$ are the ligand field energy levels. These energy levels can be placed relative to those of the separated atoms by including the first three terms in Eq. (1).

In the case of the alkaline earth monohalides, the basis functions of the M^+ center are simple one-electron orbitals. The matrix elements of the molecular Hamiltonian then become a product of the one-electron radial integrals (B_{k0}) and angular integrals [$c^k(lm,l'm')$, Gaunt coefficients]. This case differs significantly from the single-configuration ligand field theory used for polyhedral coordination complexes where the only configuration considered is d^n or f^n and the Russell–Saunders terms of this configuration are split and mixed by the ligand field. Each electronic state in these

diatomic molecules corresponds to a linear combination of one-electron configurations, $n_i l_i$ ($n = 3,4,5$ and $l = s,p,d,f$). Three kinds of terms appear in H^{CF}:

(i) terms which have the effect of rearranging the energy order of the $n_i l_i$ free M^+-ion orbitals

$$B_{00}(n_i l_i, n_i l_i; R_{MX}) = \langle n_i l_i | B_{00}(R_{MX}) | n_i l_i \rangle \; ; \tag{4}$$

(ii) terms which have the effect of lifting the spatial degeneracy ($\lambda_i = m_{l_i}$) of the $n_i l_i$ orbital

$$B_{k0}(n_i l_i \lambda_i, n_i l_i \lambda_i; R_{MX}) = \langle n_i l_i \lambda_i | B_{k0}(R_{MX}) | n_i l_i \lambda_i \rangle \; , \tag{5}$$

where $k = 2,...2l_i - 2, 2l_i$;

(iii) terms which mix both n and l but not λ:

$$B_{k0}(n_i l_i \lambda, n_j l_j \lambda; R_{MX}) = \langle n_i l_i \lambda | B_{k0}(R_{MX}) | n_j l_j \lambda \rangle \; , \tag{6}$$

where $k = |l_i - l_j|, |l_i - l_j| + 2,...l_i + l_j$.

Although the B_{00} term does not split the $2l + 1$ degeneracy of a configuration it can mix functions of the same l but different principal quantum number such as $4s$ and $5s$. The $k \neq 0$ terms of both odd and even k can mix states of different l (and n) but the same λ. These off-diagonal ligand field terms produce the mixing of one-electron orbitals whereby the metal ion is polarized. Note that this M^+ orbital polarization is treated by infinite-order degenerate perturbation theory rather than second order nondegenerate perturbation theory (which must break down when the interaction energies are comparable to the free-ion level separations). The ligand-induced polarization of M^+-ion valence and Rydberg orbitals is represented by an exactly diagonalized effective Hamiltonian matrix. This is the crucial generalization that permits a Rittner-like electrostatic model to be applied to a molecule with one electron in a highly polarizable open-shell orbital.

A key aspect of this calculation, aside from the point charge approximation, is the choice of basis functions used to describe the one electron free ion states. Since very few M^+ orbitals will be used in the basis set, an unrealistic spatial dependence of the low lying free-ion basis functions (for Ca^+: $4s$, $4p$ or $3d$) would result in very large errors.

Our goal is to construct a zero-free-parameter model for the electronic structure of the CaX molecules. The simplest choice of basis functions would be to use single exponential STO's generated from Slater's Rules[18] or hydrogenic functions generated from Burns' Rules.[19] However, neither of these functions are even approximately in agreement with Hartree–Fock $4s$, $4p$, and $3d$ orbitals. A single-exponential function cannot approximate the shape of the $3d$ orbital obtained in any of several different atomic calculations. We have selected the analytical $4s$, $4p$, and $3d$ functions reported by Weiss,[20] which are in good agreement[21] with those reported by Douglas and Garstang[22] who described the orbitals as numerical functions. This small basis can be extended to include $4d$, $4f$, $5s$, and $5p$ through the use of Ca^+ transition strengths of Treffitz as reported by Weise *et al.*[23] The method used to generate these functions is discussed in the Appendix.

The point charge approximation can be augmented by adding a point dipole located on the ligand to account for the induced dipole generated by the field of the M^+ charge. The point dipole moment μ_- can be determined from the ligand polarizability α_- and the internuclear distance R_{MX}, where

$$\mu_- = \frac{e\alpha_-}{R_{MX}^2} \; . \tag{7}$$

The quantity α_- is taken, to a first approximation, as Pauling's[24] ion polarizability. The induced point dipole contribution to the ligand field part of the Hamiltonian is then given by

$$H^{\mu^-} = -\mathscr{E}(R_{MX}) \cdot \mu_-(R_{MX}) \, , \tag{8}$$

where $\mathscr{E}(R_{MX})$ is the electric field at the X^- ion due to the valence electron. The contribution of the metal-centered valence electron to the electric field at X^- may be computed from

$$\mathscr{E}(R_{MX}) = -\frac{1}{e} \lim_{\delta \to 0} \left[\frac{H^{CF}(R_{MX}) - H^{CF}(R_{MX} + \delta)}{\delta} \right] \tag{9}$$

and the matrix elements of H^{μ^-} are

$$\langle i | H^{\mu^-}(R_{MX}) | j \rangle = \frac{\mu_-}{e} \lim_{\delta \to 0} \times \left[\frac{\langle i | H^{CF}(R_{MX}) | j \rangle - \langle i | H^{CF}(R_{MX} + \delta) | j \rangle}{\delta} \right] . \tag{10}$$

The selection rules for matrix elements of H^{μ^-} are identical to those for H^{CF}, thus λ remains a good quantum number. Matrix elements of H^{μ^-} (on the order of 0.5 eV for F^- in CaF) can then be added to the point charge Hamiltonian. The term $\mu_-^2 / 2\alpha_-$, the quasielastic energy stored in the induced dipole, is the same for all molecular electronic states at this level of approximation and therefore need not be included in the calculation of the relative energies.

The prescription for the ligand field model calculation is as follows. Given the free ion energy levels (known from atomic spectra), the eigenvalues and eigenfunctions of

$$H(R_{MX}) = H^{CF}(R_{MX}) + |i\rangle E_i^{FI} \langle i| + H^{\mu^-}(R_{MX}) \, , \tag{11}$$

with or without H^{μ^-}, may be obtained at any value of R_{MX}. Note that the model includes both diagonal and off-diagonal matrix elements of H^{CF} and H^{μ^-} in the M^+ orbital basis. The eigenfunctions of Eq. (11) are linear combinations of the one-electron free-ion wave functions.

We compare our calculated results with experimental energy levels, electric dipole transition moments, permanent electric dipole moments, matrix elements of the L^+ operator as derived from Λ doubling, spin-orbit splittings, ionization potentials, and dissociation energies. Our model is free of adjustable parameters and relies only on experimental free Ca^+ ion energy levels and transition strengths, *ab initio* orbitals *for the free* Ca^+ *ion*, and the known equilibrium bond lengths of the CaX molecules. The ionization and dissociation energies require prior knowledge of the ground state vibrational frequency of the MX molecule. We demonstrate that calcium monohalide molecules can be understood within a simple electrostatic picture and that many molecular properties may be derived from M^+-localized orbitals mixed by simple electrostatic interactions.

The results in the next section were obtained from three different model calculations. The calculations CP-7 and C-7 include seven free-Ca^+ basis functions ($4s$, $4p$, $3d$, $5s$, $5p$, $4d$,

$4f$). CP-7 includes the ligand polarization term $H^{\mu-}$. The C-3 calculation includes only the three valence orbitals $4s$, $4p$, and $3d$ and treats the ligand as a simple point charge.

RESULTS

The results presented in Table I compare the calculated and experimental values for the energies of the three lowest excited states $A\,^2\Pi$, $B\,^2\Sigma^+$, and $C\,^2\Pi$ of the calcium monohalides when two basis sets are used with (CP-7) and without (C-7) ligand polarization. The two calculations are in good agreement with the observed energy levels for the $A\,^2\Pi$ and $B\,^2\Sigma^+$ states. The observed and calculated values for the $C\,^2\Pi$ state are in agreement for CaF but do not reproduce the stabilization in energy as the ligand is changed from fluoride to iodide. The results for C-7 actually appear to agree better with experiment[25] than those of CP-7, but the same pattern of errors is present; the calculated energies of the excited states are about 1500 to 3500 cm^{-1} too high in energy. The small basis set calculation (C-3) produces transition energies that are in poorer agreement with experiment ($\sim$4000 cm^{-1} too high), but still with $A\,^2\Pi$ below $B\,^2\Sigma^+$ and the separation and center of gravity of these states decreasing properly from CaF to CaI.

An additional CaF calculation was done with an eleven function basis, including $5d$, $5f$, $6s$, and $6p$, to test the effect of adding Rydberg orbitals to the truncated C-7 basis. This calculation indicated that these additional functions have a negligible effect. The systematically too large $A\,^2\Pi$–$B\,^2\Sigma^+$ separations obtained in our calculations may reflect our inability to take account of an enhanced covalent contribution to the $B\,^2\Sigma^+$ state relative to the $A\,^2\Pi$.

The dissociation energies in the CaX series can be calculated using the known vibrational frequencies of the $X\,^2\Sigma^+$ ground states if the repulsive interaction of the two ions Ca^{2+} and X^- is assumed to have the form $Ae^{-R/\rho}$. The equations

$$V(R) = -\frac{2e^2}{R} + \text{I.P.(Ca)} - \text{E.A.(X)} + V_{CF}(R) + Ae^{-R/\rho} - \frac{2e^2\alpha_-}{R^4} + \frac{\mu_-^2}{2\alpha_-}, \tag{12}$$

TABLE I. Energies (cm^{-1}).[a]

	Observed[b]	CP-7	C-7	C-3
CaF				
$A\,^2\Pi$	16 526	17 998	17 978	19 622
$B\,^2\Sigma^+$	18 833	22 376	21 463	23 997
$C\,^2\Pi$	30 157	32 686	32 644	35 497
CaCl				
$A\,^2\Pi$	16 093	17 884	17 484	18 274
$B\,^2\Sigma^+$	16 849	21 408	19 317	20 210
$C\,^2\Pi$	26 498	32 612	29 626	31 275
CaBr				
$A\,^2\Pi$	15 922	17 820	17 263	17 873
$B\,^2\Sigma^+$	16 380	21 024	18 722	19 378
$C\,^2\Pi$	25 314	32 256	28 804	30 386
CaI				
$A\,^2\Pi$	15 586	17 695	16 874	17 273
$B\,^2\Sigma^+$	15 715	20 424	17 876	18 282
$C\,^2\Pi$	23 315	31 519	27 759	29 238

[a] Calculated at the equilibrium internuclear distance of the $X\,^2\Sigma^+$ state.
[b] Reference 25.

$$V(R_e) = -D_e \tag{13}$$

express the energy of the MX system relative to neutral atoms at $R = \infty$. Differentiating Eq. (12) twice with respect to R at $R = R_e$ yields

$$\left.\frac{dV(R)}{dR}\right]_{R=R_e} = \frac{2e^2}{R_e^2} + \left.\frac{dV_{CF}(R)}{dR}\right]_{R=R_e} - \frac{A}{\rho}e^{-R_e/\rho} + \frac{6e^2\alpha_-}{R_e^5} = 0, \tag{14}$$

where we have substituted the relationship in Eq. (7) into Eq. (12):

$$\frac{\mu_-^2}{2\alpha_-} = \frac{e^2\alpha_-}{2R^4} \tag{15}$$

and

$$\left.\frac{d^2V}{dR^2}\right]_{R=R_e} = -\frac{4e^2}{R_e^3} + \left.\frac{d^2V_{CF}(R)}{dR^2}\right]_{R=R_e} + \frac{A}{\rho^2}e^{-R_e/\rho} - \frac{30e^2\alpha_-}{R_e^6} = \frac{2}{R_e^2}\left(\frac{\omega_e^2}{4B_e}\right). \tag{16}$$

The relationship between

$$\left.\frac{d^2V}{dR^2}\right]_{R=R_e}$$

and ω_e and B_e is from Dunham.[26]

Equations (15) and (16) are solved for ρ and A which are then substituted into Eq. (12) to determine the dissociation energy. These results are summarized in Table II and agree satisfactorily (average error is less than 3%) with the experimental values of D_e.

The $MX \rightarrow MX^+(X\,^1\Sigma^+) + e^-$ appearance potentials can also be calculated since they are the difference between $E(v=0)_{CaX}$ and $E(v=0)_{CaX^+}$. $E(v=0)_{CaX^+}$ is given by

$$E(v=0)_{CaX^+} = -\frac{2e^2}{R_e} + \text{I.P.(Ca)} + \text{I.P.(Ca}^+\text{)} - \text{E.A.(X)} + Ae^{-R_e/\rho} - \frac{2\mu_-e}{R_e^2} + \frac{\mu_-^2}{2\alpha_-} + \frac{1}{2}\omega_e, \tag{17}$$

assuming (i) the Ca^+ centered valence electron is removed and (ii) the short-range repulsive interaction between Ca^{2+} and X^- is the same as for Ca^+ and X^-. The alternative to the first assumption would be to represent the ion as CaX^0,

TABLE II. Dissociation energies, D_e^0 (eV).

	Calc[b,c]	Obs[a]
CaF	5.57	5.52 ± 0.1
CaCl	4.15	4.10 ± 0.1
CaBr	3.54	3.20 ± 0.1
CaI	2.72	2.70 ± 0.1

[a] Reference 29(c).
[b] Experimental values used in Eqs. (12)–(16) are: I.P.(Ca), Ref. 17; E.A.(X), Ref. 27; ω_e, B_e, R_e, Ref. 10.
[c] Values for A and ρ determined from Eqs. (14) and (16), respectively: CaF (2460 eV, 0.285 Å), CaCl (3950 eV, 0.326 Å), CaBr (4731 eV, 0.3341 Å), CaI (5500 eV, 0.3539 Å).

TABLE III. Properties of the $CaX^+ X\,^1\Sigma^+$ state of the molecular ion.

	CaX, I.P. (eV)	CaX^+, R_e (Å)	CaX^+, ω_e[a] (cm^{-1})
CaF	5.68(5.57 ± 0.1)[b]	1.81	738
CaCl	5.49(5.6 ± 0.5)[c]	2.20	542
CaBr	5.53(5.6 ± 0.5)[d]	2.32	457
CaI	5.56(6.1 ± 0.3)[e]	2.51	378

[a] Calculated using Eq. (16) for $\left.\frac{d^2V(R)}{dR^2}\right]_{R=R_e}$.

[b] Experimental, Ref. 28.

[c] Experimental appearance potential, Ref. 29(a).

[d] Experimental appearance potential, Ref. 29(b).

[e] Experimental appearance potential, Ref. 29(c).

but because such a molecular valence scheme would have no monopolar ionic bonding, it would not be nearly as stable a structure for CaX^+ as is $Ca^{2+}X^-$. The MX^+ equilibrium internuclear distance is determined by solving

$$\left.\frac{dV(R)}{dR}\right]_{R=R_e} = 0 = \frac{2e^2}{R_e^2} - \frac{A}{\rho}e^{-R_e/\rho} + \frac{8e^2\alpha_-}{R_e^5}, \quad (18)$$

where A and ρ are determined from Eqs. (15) and (16) for MX. The second assumption is reasonable since the repulsive term is derived primarily from the interaction between the Ca^{2+} and X^- closed shells. The calculated MX ionization potentials, MX^+ bond lengths, and MX^+ vibrational frequencies are listed in Table III.

The electric dipole transition moments for the $A\leftarrow X$, $B\leftarrow X$, and $C\leftarrow X$ transitions can be calculated from the eigenfunctions of the Eq. (11) Hamiltonian and the transition moments of the free atomic-ion basis functions. Figure 1 shows the squared transition moments for the $A\,^2\Pi$, $B\,^2\Sigma^+$, $C\,^2\Pi\leftarrow X\,^2\Sigma$ transitions obtained from the CP-7 model and those measured in Ref. 2. The figure shows that not only does the calculation reproduce the $M^2_{AX} > M^2_{BX} > M^2_{CX}$ trend for CaF, it also represents the general trends vs ligand showing an $F^-\rightarrow I^-$ decrease in the M^2 for both $A\,^2\Pi\leftarrow X\,^2\Sigma^+$ and $B\,^2\Sigma^+\leftarrow X\,^2\Sigma^+$ transitions. The squared transition moments obtained for all three models are shown in Table IV. The small basis set calculations show the $M^2_{AX} > M^2_{BX}$ result, but the values for M^2_{AX} and M^2_{BX} from C-3 are too small.

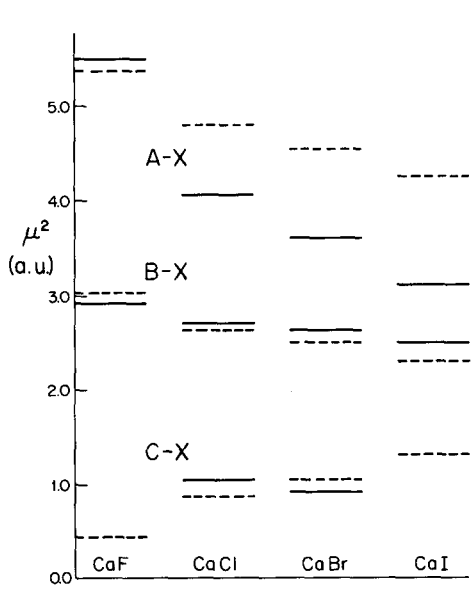

FIG. 1. The A–X, B–X, and C–X squared transition moments for the calcium monohalides compared with the experimental values from Ref. 2. Solid lines are experimental and dashed lines are calculated as described in the text.

The CaX $A\,^2\Pi$ and $B\,^2\Sigma^+$ states have often been mistakenly treated as if they were in an $l = 1$ "pure precession" relationship with each other. The ligand field model enables us to compute the relevant rotation-electronic perturbation parameters and compare them with the values obtained from the Λ doubling in the $A\,^2\Pi$ state (q),[30] the spin-rotation splitting in the $B\,^2\Sigma^+$ state (γ), and $BJ\cdot L$ $A\,^2\Pi\sim B\,^2\Sigma^+$ perturbation matrix elements (η). The parameters q, γ, and η are all related to the matrix element of L^+ between the $A\,^2\Pi$ and $B\,^2\Sigma^+$ states (in the case a, signed-Ω basis set)[31]:

$$\begin{aligned}\eta_{v_\Pi v_\Sigma} &= \langle v_\Pi|B(R)|v_\Sigma\rangle\langle {}^2\Pi_{3/2}|\tfrac{1}{2}L^+|{}^2\Sigma^+_{1/2}\rangle \\ &= \langle v_\Pi|B(R)|v_\Sigma\rangle\langle {}^2\Pi_{1/2}|\tfrac{1}{2}L^+|{}^2\Sigma^+_{-1/2}\rangle \\ &= \tfrac{1}{2}B_{v_\Pi v_\Sigma}\langle\Lambda=1|L^+|\Lambda=0^+\rangle, \end{aligned} \quad (19)$$

$$q = \sum_{v_\Sigma}\frac{2B^2_{v_\Pi v_\Sigma}|\langle\Lambda=1|L^+|\Lambda=0^+\rangle|^2}{E({}^2\Pi,v_\Pi)-E({}^2\Sigma^+,v_\Sigma)} \simeq \frac{2\overline{B}^2_v|\langle\Lambda=1|L^+|\Lambda=0^+\rangle|^2}{E({}^2\Pi,v)-E({}^2\Sigma^+,v)} = \frac{8\eta^2}{\Delta E(\Pi,\Sigma)} \quad (20)$$

$$\gamma = \sum_{v_\Pi}\frac{2B^2_{v_\Pi v_\Sigma}|\langle\Lambda=1|L^+|\Lambda=0^+\rangle|^2}{E({}^2\Sigma^+,v_\Sigma)-E({}^2\Pi,v_\Pi)} = -q. \quad (21)$$

$B_{v_\Pi v_\Sigma}$ may be replaced by

$$\overline{B}_v = \tfrac{1}{2}(B_{v_\Pi}+B_{v_\Sigma})\delta_{v_\Pi,v}\delta_{v_\Sigma,v} \quad (22)$$

because the potential energy curves for the $B\,^2\Sigma^+$ and $A\,^2\Pi$ states are nearly identical.

As pointed out by Hall *et al.*[32] and Colbourn and Wayne,[33] the L^+ operator is defined with respect to the molecular center of mass. The L^+ matrix elements can be evaluated for metal-centered basis functions by

$$\begin{aligned}&\langle {}^2\Pi_{3/2}|L^+|{}^2\Sigma^+_{1/2}\rangle \\ &\quad = \langle\Lambda=1|l^+|\Lambda=0\rangle - \mu_L\langle {}^2\Pi|R_e\nabla_i|{}^2\Sigma\rangle, \end{aligned} \quad (23)$$

TABLE IV. Transition moments, M^2 (a.u.).[a]

	Observed	CP-7	C-7	C-3
CaF				
A–X	5.47	5.38	4.81	3.38
B–X	2.94	3.01	2.73	1.61
C–X	...	0.43	0.86	0.71
CaCl				
A–X	4.07	4.80	3.57	2.74
B–X	2.70	2.62	2.15	1.43
C–X	1.05	0.86	1.84	1.66
CaBr				
A–X	3.58	4.58	3.19	2.48
B–X	2.62	2.50	2.00	1.38
C–X	0.93	1.04	2.16	1.96
CaI				
A–X	3.10	4.25	2.61	2.10
B–X	2.49	2.33	1.76	1.29
C–X	...	1.32	2.64	2.40

[a] $1.0\ (a.u.)^2 = 6.46\ (D)^2$.

where l^+ is the one-electron raising operator centered on the metal ion, $\mu_L = M_L/(M_{Ca} + M_L)$, R_e is the equilibrium internuclear distance, and ∇_i is the one electron gradient operator.[34] Table V presents the observed and calculated values of η. The center of mass transformation term in Eq. (23) makes a correction of $\sim 10\%$ to the Ca^+-centered matrix element of l^+.

These results for the η parameter provide another confirmation of the ligand field model for the wave functions of the $A\,^2\Pi$ and $B\,^2\Sigma^+$ states. If the calculated wave functions did not contain the proper amounts and relative phases of p and d Ca^+-ion basis functions, the rotation-electronic parameters (q, γ, η) could not have been reproduced so accurately.

The spin-orbit splitting in the $A\,^2\Pi$ and $C\,^2\Pi$ states of the calcium monohalides has been used to test previous models for the electronic structure of the alkaline earth monohalides. The spin-orbit splittings in the CaX $A\,^2\Pi$ states

$$A(^2\Pi) = \langle {}^2\Pi_{3/2}|H^{SO}|{}^2\Pi_{3/2}\rangle - \langle {}^2\Pi_{1/2}|H^{SO}|{}^2\Pi_{1/2}\rangle = a_\pi \tag{24}$$

correspond to a_π values of 71 (CaF), 67 (CaCl), 59 (CaBr), and 45 cm^{-1} (CaI). The molecular spin-orbit parameter a_π would be equal to the free atomic ion parameter ζ_{nl} if

$$|A\,^2\Pi\rangle = |Ca^+ nl\pi\rangle .$$

These a_π values are intermediate between $\zeta_{4p} = 148$ cm^{-1} and $\zeta_{3d} = 25$ cm^{-1}, suggesting that the CaX $A\,^2\Pi$ state is a linear combination of $4p\pi$ and $3d\pi$. The behavior of the $C\,^2\Pi$ spin-orbit splitting is curious. For CaF, $a_\pi = 29$ cm^{-1} suggests that the $C\,^2\Pi$ state arises from a pure $3d\pi$ orbital. However, a_π for $C\,^2\Pi$ is very ligand sensitive and rises to $a_\pi = 428$ cm^{-1} for CaI.

The spin-orbit Hamiltonian is

$$H^{SO} = \sum_i \frac{1}{2\mu^2c^2}\frac{1}{r_i}\frac{\partial U(r_i)}{\partial r_i}(\mathbf{l}_i \cdot \mathbf{s}_i) = \sum_i a_i(r_i)\mathbf{l}_i \cdot \mathbf{s}_i . \tag{25}$$

The center-of-mass transformation term is much less important for H^{SO} than for L^+ [32] and is neglected here.

If we consider only $\Delta\Lambda = 0$ spin-orbit matrix elements for the molecular states

$$|^2\Pi\rangle = \sum_j C_j|n_j l_j \lambda = 1\rangle \tag{26}$$

$$\langle {}^2\Pi_{3/2}|H^{SO}|{}^2\Pi_{3/2}\rangle = \sum_{j,k} C_j C_k^* \langle n_k l_k \lambda = 1, \sigma = \tfrac{1}{2}|a\mathbf{l}_z\mathbf{s}_z|n_j l_j \lambda = 1, \sigma = \tfrac{1}{2}\rangle = \sum_j |C_j|^2 \tfrac{1}{2}\zeta_{n_j l_j} + \sum_{k\neq j} C_j C_k^* \tfrac{1}{2}\langle n_k l_j|a|n_j l_j\rangle . \tag{27}$$

The one-electron radial integral a_π is then a weighted sum of the ζ_{nl} of the basis functions and the $\langle nl|H^{SO}|n+1l\rangle\Delta l = 0$ cross terms. Although the radial wave functions used in this calculation are inadequately accurate to compute the individual ζ_{nl} values, the ζ_{nl} can be determined from the spin-orbit splittings observed in the free ion.

$$\zeta_{np} = \tfrac{2}{3}[\langle np^2P_{3/2}|H^{SO}|np^2P_{3/2}\rangle - \langle np^2P_{1/2}|H^{SO}|np^2P_{1/2}\rangle],$$
$$\zeta_{nd} = \tfrac{2}{5}[\langle nd\,^2D_{5/2}|H^{SO}|nd\,^2D_{5/2}\rangle - \langle nd\,^2D_{3/2}|H^{SO}|nd\,^2D_{3/2}\rangle] . \tag{28}$$

The cross terms, however, are neither accessible from free-ion spectra, nor evaluable from our free-ion basis functions. Correct evaluation of these matrix elements would depend critically on an accurate representation of the wave functions in the region of the nucleus, an inadequacy of even very elaborate *ab initio* calculations. The cross term $\langle 4p|H^{SO}|5p\rangle$ is expected to be important since the values of ζ_{4p} and ζ_{5p} are both appreciable (148 and 50 cm^{-1}, respectively), but we have no unbiased way of evaluating it. Thus, although the ligand field eigenfunctions should be capable of accounting for the $A\,^2\Pi$ state spin-orbit constant, the value calculated by ignoring cross terms is unlikely to be accurate.

The spin-orbit splittings of the $A\,^2\Pi$ and $C\,^2\Pi$ states were calculated either by assuming that the $4p/5p$ and $3d/4d$ cross terms are zero or by arbitrarily setting them to the average of the nl and $(n+1)l$ values observed from the atomic spectra. The observed and calculated values are compared in Table VI. The results for the $A\,^2\Pi$ state, assuming the cross term is zero, account for approximately half of the apparent reduction in the spin-orbit parameter from ζ_{4p} to a_π and also the trend vs halide ligand, but the agreement with experimental values is inferior to that obtained for other observables. The results for the $C\,^2\Pi$ state are acceptable for CaF, but completely at variance with the trend vs ligand.

TABLE V. Lambda doubling.

	η (cm^{-1})		
	Observed	Calc[c] (uncorrected)[b]	Calc[c] (corrected)
CaF	0.296[a]	0.292	0.312
CaCl	0.123[a]	0.138	0.151
CaBr	0.080[a]	0.087	0.099
CaI	0.062	0.062	0.076

[a] Determined from q using Eq. (20).
[b] Not corrected for center of gravity shift [Eq. (23)].
[c] From the CP-7 model calculation.

TABLE VI. Spin-orbit splitting—a_π (cm^{-1}).

		Observed	Calc[a,c]	Calc[b,c]
CaF	$A\,^2\Pi$	71	109	83
	$C\,^2\Pi$	29	46	12
CaCl	$A\,^2\Pi$	67	101	82
	$C\,^2\Pi$	76	54	5
CaBr	$A\,^2\Pi$	59	98	81
	$C\,^2\Pi$	223	59	11
CaI	$A\,^2\Pi$	45	92	78
	$C\,^2\Pi$	428	67	22

[a] Setting the $nl \sim (n+1)l$ matrix elements of H^{SO} to zero.
[b] Setting $nl \sim (n+1)l$ matrix elements to $\frac{1}{2}(\zeta_{nl} + \zeta_{(n+1)l})$.
[c] CP-7 model calculation.

In fact, no combination of metal orbitals can account for the spin-orbit splitting observations in the $C\,^2\Pi$ state of CaBr and CaI because the largest a_π derived exclusively from Ca^+ orbitals would be $a_\pi = 148\ cm^{-1}$, corresponding to a CaX orbital composed entirely of Ca^+ $4p\pi$. The polarization of the $C\,^2\Pi$ state is very different from that of the $X\,^2\Sigma^+$, $A\,^2\Pi$, and $B\,^2\Sigma^+$ states as will be discussed later. It is possible that much of the spin-orbit splitting in the $C\,^2\Pi$ state of CaBr and CaI comes from the interaction of the valence orbital with the large nuclear charge of these ligands.

The permanent electric dipole moments of CaF,[14] CaCl,[12] and CaBr[13] in the $X\,^2\Sigma^+$ ground states have been measured to be 3.07(7), 4.26(2), and 4.364(20) D using laser rf (CaF) or laser microwave (CaBr, CaCl) methods. These quantities can be determined within the ligand field model by calculating the Ca^+-centered orbital dipole moment of the CaX ground state and adding it to the Ca^+/X^- point charge dipole and the induced dipole moment for the ligand μ_- used in the polarization calculation. So, as an example,

$$\mu_{CaF} = eR_e + \mu_{Ca^+} + \mu_{F^-}\,, \tag{29}$$

where

$$\mu_{Ca^+} = \langle\psi(Ca^+)|er|\psi(Ca^+)\rangle = -1.98 \text{ a.u. (for CaF } X\,^2\Sigma^+)\,, \tag{30}$$

$$\mu_{F^-} = -\alpha_- \frac{e}{R_e^2} = -0.52 \text{ a.u.}\,, \tag{31}$$

$$eR_e = 3.69 \text{ a.u.}\,, \tag{32}$$

giving a value of 3.01 D in good agreement with the experimental value. The same method results in the following calculated values for the $X\,^2\Sigma^+$ states: CaCl (3.89 D), CaBr (4.21 D), and CaI (4.62 D). The $|\psi(Ca^+)\rangle$ wave function in Eq. (30) is not the symmetrized wave function for the CaF molecule, which must give a value of zero for this matrix element because of parity. It is the lowest eigenfunction of the ligand field Hamiltonian for Ca^+ including the strong inhomogeneous electric field of the F^- ligand.

In addition to comparing our results to experimental values, we can examine them in relation to the results of much more sophisticated molecular orbital calculations. Childs *et al.*[8] have performed an $X\alpha$-SCF calculation on CaF from which they obtain the orbital composition of the $X\,^2\Sigma^+$, $A\,^2\Pi$, and $B\,^2\Sigma^+$ states. Honjou *et al.*[9] have calculated a variety of properties of CaCl including a Mulliken population analysis of the molecular orbitals, molecular dipole moments, and transition moments. Table VII compares the transition moments and dipole moments of the low lying states of CaCl with those obtained by this *ab initio* calculation and reports the corresponding values calculated from the ligand field model for the other calcium monohalides. It is clear that the simple ligand field model incorporates many of the general orbital mixing characteristics obtained in this accurate and elaborate *ab initio* calculation.

TABLE VII. CaX transition and permanent dipole moments (a.u.).[a]

	CaF	CaCl[b]	CaBr	CaI
X, X	1.18	1.52 (1.53)	1.65	1.82
A, A	1.61	1.89 (1.49)	2.00	2.13
B, B	2.25	2.45 (1.82)	2.54	2.66
C, C	3.24	3.79	3.97	4.16
A, B	0.58	0.67 (0.44)	0.69	0.72
X, A	2.32	2.19 (2.34)	2.14	2.06
X, B	1.73	1.62 (1.87)	1.58	1.53
X, C	0.66	0.92	1.02	1.15

[a] CP-7 calculation.
[b] Values in parentheses from Ref. 9.

The wave functions obtained in the CP-7 calculation are presented in Table VIII for the $X\,^2\Sigma^+$, $A\,^2\Pi$, $B\,^2\Sigma^+$, and $C\,^2\Pi$ states in all four of the calcium monohalides. They are expressed in terms of the percentage composition of the single center basis functions. In the *X*, *A*, and *B* states it is clear that the three low lying orbitals 4*s*, 4*p*, and 3*d* are by far the dominant basis functions. The *C* state has a very different composition than the *X*, *A*, and *B* states. The model represents the $C\,^2\Pi$ state less well than the lower states as indicated by its failure to predict the substantial stabilization as $F^- \rightarrow I^-$ (Table I). The polarization of the valence π orbital *toward* the ligand in the $C\,^2\Pi$ state suggests that this state will be much more susceptible to covalent effects than the other low lying states.

The orbital composition of the $X\,^2\Sigma^+$ state is almost identical in all four molecules, being about 80% 4*s* with 20% 4*p* polarizing it away from the ligand. There is some 5*s* character which represents a slight expansion of the orbital. The composition of the $A\,^2\Pi$ state is also similar for all four CaX molecules. $A\,^2\Pi$ has more than 50% 4*p* character as anticipated by others based on the spin-orbit splitting, but the 3*d* and 4*d* character is nonnegligible, thus polarizing the valence orbital away from the ligand as in the ground state. These results demonstrate that although the $A\,^2\Pi$ state is mainly composed of the 4*p* orbital, the $B\,^2\Sigma^+$ state is not and that these two states are not an $l = 1$ pure precession complex. $B\,^2\Sigma^+$ is primarily 3*d* and becomes more so as the halide is changed to I^-. It has less than 10% 4*s* character but possesses a considerable 4*p* contribution which polarizes it away from the ligand as in the *X* and *A* states, although to a lesser extent. The $C\,^2\Pi$ state is mostly 5*p* in CaF but acquires

TABLE VIII. Wave functions: Orbital mixing percentages.

		4*s*	4*p*	3*d*	Rydberg[c]
CaF[a]	*X*	77(81)	20(13)	0(3)	3
	A	...	69(52)	24(47)	7
	B	9(1)	38(37)	42(54)	11
	C	...	4	26	70
CaCl[b]	*X*	79(78)	19(21)	0(1)	2
	A	...	62(72)	32(27)	6
	B	7(6)	32(34)	54(61)	7
	C	...	17	43	40
CaBr	*X*	80	19	0	1
	A	...	60	35	5
	B	6	31	57	6
	C	...	23	47	30
CaI	*X*	81	18	0	1
	A	...	55	41	4
	B	5	28	62	5
	C	...	32	49	19

[a] Values in parentheses are those reported in Ref. 8.
[b] Values in parentheses are those reported in Ref. 9.
[c] Leading Ca^+ Rydberg orbital contributions to the *X*, *A*, *B*, and *C* CaX states, respectively, are 5*s*, 5*p*, 4*d*, and 5*p*.

increasing $4p$ and $3d$ character as F→I. These $4p$ and $3d$ basis orbitals have mixed so as to polarize the wave function toward the ligand. This polarization toward the ligand may account for the puzzling behavior of the spin-orbit splitting in this state. With a portion of the Ca^+ valence orbital located near the ligand nucleus, the electron experiences a relativistic interaction with this nucleus as well. Therefore, the spin-orbit splitting, which is small for CaF as expected for an interaction with a F ($Z = 9$) nucleus, increases to greater than 400 cm^{-1} at the high-Z limit CaI ($Z = 53$). Note that this increase in spin-orbit interaction cannot arise from significant covalent Ca^+I^- configurational character, because then the unpaired electron would be in a more than half filled $5p\pi$ orbital on iodine. The result would be a large spin-orbit splitting with an *inverted* pattern, placing $C\,^2\Pi_{3/2}$ below $C\,^2\Pi_{1/2}$.

The compositions of the CaX semiempirical ligand field wave functions compare favorably with those reported in the more elaborate *ab initio* calculations on CaF and CaCl. The results from the $X\alpha$-SCF calculation on CaF are in parentheses in Table VIII. The agreement for the $X\,^2\Sigma^+$ and $B\,^2\Sigma^+$ states is very good (for $B\,^2\Sigma^+$, when our $3d$ and $4d$ fractional characters are combined to produce an overall d percentage of 53%). The $A\,^2\Pi$ state is seen to be primarily $4p\pi$ with 20%–40% $3d$ character depending on the ligand. The MCSCF wave functions for CaCl and the simple ligand field results are in excellent agreement for the X, A, and B states.

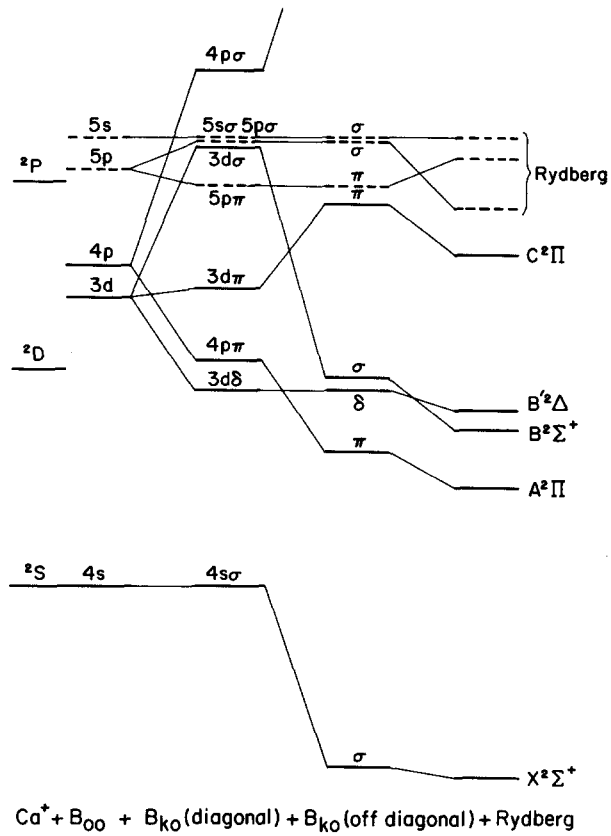

FIG. 2. The effects of the various terms in the ligand field C-7 model shown relative to the energies of the first three free Ca^+-ion states. The overall upward shift of all orbital energies by 6.6 eV due to the B_{00} term has been omitted but the shifts relative to the $4s$ orbital energy are shown.

DISCUSSION

The ligand field model presented here accounts, with zero free parameters, for a wide variety of properties of the alkaline earth monohalide molecules. The model provides an intuitively useful representation of how the global MX electronic structure depends on internuclear distance, halide polarizability, and free-M^+ ion electronic structure. Simple, explicitly identified electrostatic effects cause intermixing among the relatively compact ($\langle r\rangle_{nl} \approx R_e$) $4s$, $4p$, $3d$ valence basis orbitals, some admixture of larger Rydberg orbitals into the MX valence states, and polarization of the ligand.

Figure 2 shows how the various terms in the ligand field Hamiltonian for CaF shift the free-ion energy levels and mix the free-ion nl orbitals. The figure also illustrates why a degenerate perturbation theoretic treatment is essential. The free-ion energy levels are shifted by the diagonal B_{00} term which reorders the various one-electron configurations. The free-ion $nl\,^2L$ terms are split by the $k \neq 0$ diagonal B_{k0} terms into molecular states associated with σ, π, and δ orbitals. The energy levels at this stage are still not representative of the experimental values. Extensive configurational mixing is necessary to represent properly the low lying states. When the off-diagonal ligand field terms are included, the largest of which is B_{10}, which mixes $4p$ with $3d$ and $4s$, the lowest energy σ and π molecular orbitals become strongly polarized away from the ligand. Both point charge and ligand induced dipole μ_- terms can be off-diagonal and contribute to orbital polarization on the metal center. Within the $4s$, $4p$, $3d$ basis this level of treatment begins to approximate the energy level structure, but the excited states remain too high and the transition moments too small (C-3, Tables I and IV). It is necessary to expand the basis set to contain the $(n + 1)l$ and $4f$ orbitals, which result in a markedly enhanced agreement of the C-7 calculation with the experimental values.

The mixing of $(n + 1)l$ Rydberg orbitals into the valence orbitals is a measure of how the M^+ orbitals expand to accommodate the repulsive electrostatic interaction with the X^- ligand. The resultant MX valence orbital looks more like that of the neutral metal atom than that of the free M^+. This valence orbital expansion leads to a reduction of spin-orbit splittings, increased polarizability, and large electric dipole transition moments. Multiligand coordination complexes do not exhibit significant $nl \sim (n + 1)l$ mixing because, in an octahedral system, orbital expansion would increase the electron density near ligands, thus increasing the energy of the system. In the diatomic molecule, there is only one negatively charged ligand so that by expanding ($\Delta l = 0$) and polarizing ($\Delta l = 1$) the M^+ orbitals the electron density can be effectively moved away from the X^- ligand. These two effects, expansion through mixing in of Rydberg orbitals and polarization through mixing of valence orbitals are consequences of a simple, degenerate perturbation theoretic, electrostatic model that have not been included in previous attempts to describe the alkaline earth monohalide molecules.

The ligand dependence of the relative $3d$ and $4p$ character in the A and B states, a monotonic increase in $3d$ character in both states as $F^-\rightarrow I^-$, is easily explained by the ligand

field model. The $3d\ ^2D$ and $4p\ ^2P$ states of the free Ca^+ ion lie at 13 690 and 25 350 cm^{-1}. As the strength of the ligand field is increased (moving the X^- charge to shorter internuclear distance) the 3*d* and 4*s* orbitals, which are more compact than 4*p*, are destabilized by the B_{00} terms relative to 4*p*. Thus the 4*p* basis function character in the *X*, *A*, and *B* states will be larger for the strong field of the fluoride ion than that of I^-. The overall stabilization for the $B\ ^2\Sigma^+$ and $A\ ^2\Pi$ states of CaI relative to CaF is also consistent with this picture. As the field is weakened, the MX states look more like the free Ca^+ 3*d* orbital and therefore the energies of the *A* and *B* states above $X\ ^2\Sigma^+$ tend toward the free Ca^+ 3*d*-4*s* energy separation of 13 690 cm^{-1}.

The effects of ligand polarization have been examined because the ligand orbitals are strongly polarized toward the metal center, thereby shifting the center of negative charge and effectively increasing the ligand field. The crude way this X^- polarizability has been treated here may be insufficiently accurate to improve on the simple point charge model. The most important neglected polarization effect and the most difficult to include in the present calculation is saturation of the X^- induced dipole moment μ_-. This saturation can result from higher order terms in the polarization expansion and from overlap repulsion effects, as discussed by Brumer and Karplus.[35] In addition to the neglect of μ_- saturation effects, the electric field at the ligand due to the Ca^+ ion has been oversimplified as e/R_e^2. In fact, the M^+ electric field which induces the X^- dipole should be that of Ca^{2+} minus that of the ligand field mixed Ca^+-centered orbital which is

$$\frac{1}{e}\frac{dE_{CF}}{dR}\Big]_{R=R_e}$$

[see Eq. (9)]. Since

$$\frac{dE_{CF}}{dR}\Big]_{R=R_e}$$

is different for each low lying state, the expression for the electric field at the ligand should be corrected for each state. However, saturation effects will diminish this distinction between MX electronic states. The best approximation may be to use the same induced ligand dipole, essentially saturated, in all states for a given ligand.

Another approximation that has been made is the choice of Pauling's polarizabilities. Other somewhat smaller values[35,36] have been suggested, but they all fall in the range of the simple α's suggested by Pauling. In view of the other approximations in our treatment of ligand polarization, our arbitrary choice of Pauling's values does not significantly affect the quality of the results.

One factor that has been neglected at this level of the model is the inclusion of Ca^{2+} core polarization by the X^- electric field. The $\alpha_{Ca^{2+}}$ has been calculated to be about 0.54 $Å^3$ [36] which, in the field of the X^- negative charge, would make an additional contribution to the molecular permanent dipole moment of -0.67 D for CaF. However, the induced dipole moment from the interaction of this same center with the *polarized* valence electron is similar in magnitude but opposite in sign ($+0.69$ D for CaF) to that due to the X^- charge, thus making the net effect of the Ca^{2+} core polarizability small.

There has been considerable interest in the energy and other properties of the lowest $^2\Delta$ state of the alkaline earth monohalides. This state has not been observed for any of the alkaline earth monohalides except BaCl,[37] but is known for the isoelectronic Group IIIb oxides ScO,[38] YO,[38] and LaO.[39] The $\Lambda = 2$ ligand field matrix can be diagonalized to yield the energy, orbital composition, and other properties of this $^2\Delta$ state for the CaX molecules (see Table IX). The $^2\Delta$ state is almost entirely of $3d\delta$ orbital character with a very slight admixture of $4f\delta$ which polarizes it away from the ligand. The molecular spin-orbit one-electron parameter $a_\delta = 2A(^2\Delta)$ should be approximately equal to $\zeta(Ca^+, 3d) = 24\ cm^{-1}$. The $^2\Delta$ state should have a substantial electric dipole moment. Unfortunately, the predicted location of this $^2\Delta$ state at about 24 000 cm^{-1} will make its observation by OODR excitation or fluorescence spectroscopy difficult. When the $^2\Delta$ state is observed it will serve as a good test of the present ligand field model.

With *ab initio* wave functions for the valence orbitals of the free Sr^+ and Ba^+ ions, this ligand field model should produce results of comparable quality to those presented here for Ca^+. It will be interesting to apply this model to the magnesium monohalide molecules. For MgX, covalent configurations will be lower in energy than for CaX because I.P.(Mg) is 1.5 eV higher than I.P.(Ca).

CONCLUSION

The ligand field approach presented here, using the point charge Hamiltonian, which requires and incorporates a detailed understanding of the free atomic ion structure, predicts a wide variety of molecular properties for all of the low lying formally ionic states. The critical features in the evaluation of the Hamiltonian are the inclusion of the monopolar B_{00} term and the use of degenerate perturbation theory to obtain results with the multiconfigurational basis. The monopolar term (B_{00}) is an extremely important and previously neglected feature of the multiconfigurational ligand field approach. Configurations such as Ca^+ 4*p*, with electrons in orbitals whose radial extent is greater than that of the metal-ligand internuclear distance, are stabilized relative to those configurations in which electrons reside in contracted, core-like orbitals, such as Ca^+ 3*d*. This configurational

TABLE IX. Properties[a] of the CaX $B'\ ^2\Delta$ state.

	CaF	CaCl	CaBr	CaI
T_e	24 950	22 960	22 310	21 380
$\mu(B'\ ^2\Delta)$ Debye	7.57	8.40	8.71	9.55
Spin-orbit a_δ (cm^{-1})	27	28	29	29
$M^2(B'\ ^2\Delta - A\ ^2\Pi)$ $(a.u.)^2$	3.09	2.48	2.30	2.03
[b] $\nu_{00}(B'-A)$ (cm^{-1})	8 424	6 867	6 388	5 794
$M^2(B'\ ^2\Delta - C\ ^2\Pi)$ $(a.u.)^2$	0.08	0.39	0.55	0.90
[b] $\nu_{00}(C-B')$ (cm^{-1})	5 207	3 538	3 004	1 935

[a] From CP-7 calculation.
[b] Determined from experimental $A\ ^2\Pi$ and $C\ ^2\Pi$ T_e and the calculated T_e of $B'\ ^2\Delta$.

reordering effect explains the dominant $4p\pi$ character in the $A\,^2\Pi$ state of the CaX molecules. This large/small orbital configurational reordering has also been observed for the low lying states of the rare earth oxides.[40,41]

The degenerate perturbation theory treatment is necessary in the accurate evaluation of this Hamiltonian because individual orbitals (4*s*, 4*p*, and 3*d* primarily) are connected by electrostatic matrix elements that can be larger than the zero order energy separations. These atomic orbitals are therefore greatly mixed in the CaX molecules, resulting in polarization of the metal-centered orbitals, but not to the extent that a second order approach that does not allow for saturation would indicate.

A model based on atomic polarizability α_+ has an M^+ induced dipole moment $\mu_+ = \alpha_+ \mathscr{E}^-$, which varies linearly with ligand electric field at all internuclear distances. In order to arrive at this expression in which α_+ is not a function of $\mathscr{E}^-$, the mixing of $\Delta L = 1$ atomic states which produces the polarization must come from a second order perturbation treatment.[42] This approximation breaks down when the matrix elements connecting these atomic states approach the magnitude of the zero order energy level separations. As a consequence, a model describing any molecular property, particularly one involving excited states, must incorporate the nonlinearity of the polarization of Ca^+ as a function of electric field. The direct diagonalization of the point charge Hamiltonian explicitly accounts for this nonlinearity present at the high electric field generated by the ligand.

It should be possible to apply this model to many other ionic diatomic molecules. Of special interest are the transition element oxides, and rare earth monohalides and monohydrides. Several problems remain to be solved, particularly those stemming from large ligand polarizabilities (hydrides, oxides), multiple oxidation states (oxides), and metal centers which have high ionization potentials (transition elements). This implies that, for transition metal monohalides and monohydrides, low lying $M^\circ X^\circ$ configurations could severely affect the results for all the properties presented here. For metal oxides, there are two additional classes of configurations which must be considered, $M^\circ O^\circ$ and M^+O^+, both of which possess an open shell on the ligand. The utility of an $M^{2+}O^{2-}$ approach for the transition metal oxides, where the second ionization potentials for the metals are high, is questionable. However, the similarity of the electronic structure and spectrum of ScO to CaF (two isoelectronic species) is encouraging evidence that the $M^{2+}O^{2-}$ valence structure may lend itself to a parametrization similar to that of the spectrochemical series developed for inorganic coordination complexes. The failure of a single valence ligand field model should be readily identifiable because it will be reflected by large variations in the B_e and ω_e molecular constants among states close in energy.

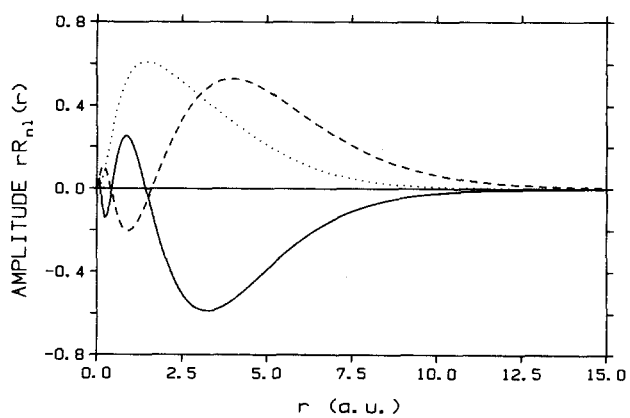

FIG. A1. Radial wave functions $rR_{nl}(r)$ from Ref. 20 used in the ligand field calculations for: 4*s* (solid), 4*p* (dashed), and 3*d* (dotted).

We have applied a simple model for the electronic structure of the alkaline earth monohalides which is based explicitly on a point charge approximation. Many properties of the low lying electronic states have been predicted quantitatively and ligand dependent trends have been explained. This simple electrostatic model, whereby the metal centered atomic orbitals are mixed by a point charge, accounts for the general features of the electronic structure of these highly ionic molecules.

The quantitative accuracy of this model will be degraded by covalent bonding effects or large ligand polarizabilities. However, as is the case with ligand field theory in coordination complexes, such a model provides a direct relationship between the free metal ion and molecular electronic structure, thus making it possible to use the well developed concepts of atomic periodicity to explain the electronic properties of a wide variety of molecules.

ACKNOWLEDGMENTS

We thank Professor P. Bernath, Professor J. Schamps, and Professor T. Törring, Dr. M. Dulick, and Dr. W. Ernst for valuable insights and criticism. This work was supported by a grant from the National Science Foundation (CHE81-12966).

APPENDIX

The Ca^+ 4*s*, 4*p*, and 3*d* radial functions of Weiss[20] are shown in Fig. A1. These functions were used in the C-3 model as well as in the larger basis set calculations. Although Treffitz calculated the higher energy orbitals 4*d*, 4*f*, 5*s*, and 5*p*, only the transition strengths between these and the 4*s*, 4*p*, and 3*d* orbitals are reported in Ref. 23. In order to include the 4*d*, 4*f*, 5*s*, and 5*p* functions in the ligand field calculation, it was necessary to generate approximations to these functions.

The 4*s*, 4*p*, and 3*d* functions were available as linear combinations of Slater-type orbitals (STO's)

$$\phi_{nl}(r) = \sum_i C_i \chi_i(r)\,, \tag{A1}$$

where

$$\chi_i(r) = \frac{(2\alpha)^{n+1/2}}{[(2n)!]^{1/2}}\, r^{n-1} e^{-\alpha r}\,. \tag{A2}$$

We have assumed the functional form of $\phi_{(n+1)l}$ to be

$$\phi_{(n+1)l} = C_1 \phi_{nl} + C_2 \frac{(2\alpha')^{n+3/2}}{[2(n+1)!]^{1/2}}\, r^n e^{-\alpha' r}\,.$$

$\phi_{(n+1)l}$ is a linear combination of ϕ_{nl} and a STO with the principal quantum number incremented to $n+1$ and a new adjustable α' exponential parameter. The three equations

$$\int_0^\infty \phi^2_{(n+1)l} r^2\, dr = 1 \qquad \text{(normalization)}, \quad \text{(A3)}$$

$$\int_0^\infty \phi_{(n+1)l}\phi_{nl} r^2\, dr = 0 \qquad \text{(orthogonality)}, \quad \text{(A4)}$$

and

$$\left| \int_0^\infty \phi_{(n+1)l} r \phi_{n'l'} \right|^2 = \frac{S_{(n+1)l,n'l'}}{2l_>}$$

(transition moment), (A5)

where $l_>$ is the larger value of l and l'[43] can be solved numerically to determine C_1, C_2, and α'. This procedure generates the $4d$ and $5s$ orbitals because *ab initio* values of $S_{4p,5s}$ and $S_{4p,4d}$ have been reported.[23] Once ϕ_{5s} is generated, $S_{5s,5p}$ can be used to generate ϕ_{5p}. ϕ_{4f} is created from a single exponential STO by adjusting α_{4f} to satisfy Eq. (A5) with the *ab initio* value of $S_{3d,4f}$. These radial functions are displayed in Fig. A2. The relative phases of the radial functions ϕ_{nl} are not important in the ligand field calculation, provided that these phases and the signs of the radial integrals used in evaluating quantities such as transition moments are defined consistently throughout.

It was not our purpose to calculate the best Hartree–Fock functions for the Rydberg orbitals of Ca^+. The goal was to obtain orbitals with approximately correct shapes in the region of space that is most sensitive to the ligand field radial operators. Only one or two lobes of these radial functions must be scaled approximately correctly. We have ensured that this is true by scaling our orbitals to reproduce the Ca^+ transition strengths. These are determined by Eq. (A5), which samples the same region as the ligand field parameters [Eqs. (4)–(6)]. In fact, when $4s$ and $4p$ are approximated as single STO's forced to match the first moment of the functions in Ref. 20, thus ignoring the internal nodal structure, the results from a ligand field calculation using such orbitals are very similar to those reported in this paper.

Our greatest concern with this method of generating Rydberg orbitals is in the shape of the $4d$ orbital which appears to have an oversized inner lobe, leading to $\langle r^n \rangle$ $(n > 0)$ moments which are smaller than those of $4p$. This is unusual for what should be a Rydberg orbital. However, when a larger $4d$ orbital is used, such that its $\langle r^n \rangle$ moments are intermediate between those of $4p$ and $4f$ but its S_{4p4d} is about 10% larger than that reported in Ref. 23, the results for CP-7 and C-7 remain essentially unchanged.

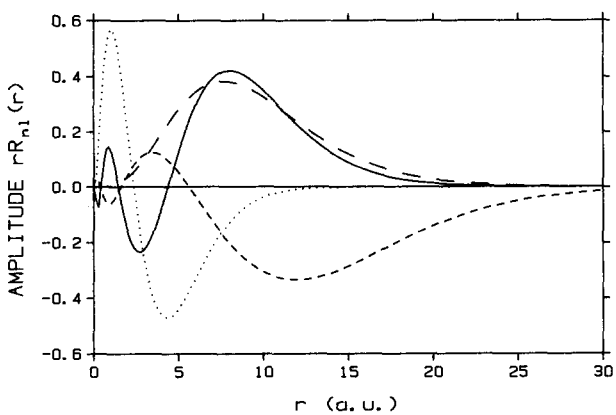

FIG. A2. Radial wave functions $rR_{nl}(r)$ calculated as described in the Appendix: $5s$ (solid), $5p$ (small dashed), $4d$ (dotted), and $4f$ (large dashed).

[1] L. B. Knight, Jr., W. C. Easley, W. Weltner, Jr., and M. Wilson, J. Chem. Phys. **54**, 322 (1971).
[2] P. J. Dagdigian, H. W. Cruse, and R. N. Zare, J. Chem. Phys. **60**, 2330 (1974).
[3] T. Dunn, in *Physical Chemistry: An Advanced Treatise*, edited by H. Eyring (Academic, New York, 1970), Vol. 5, p. 205.
[4] P. F. Bernath, B. Pinchemel, and R. W. Field, J. Chem. Phys. **74**, 5508 (1981).
[5] L. Klynning and H. Martin, Phys. Scr. **24**, 33 (1981).
[6] E. S. Rittner, J. Chem. Phys. **19**, 1030 (1951).
[7] T. Törring and W. E. Ernst, J. Chem. Phys. **81**, 4614 (1984).
[8] W. J. Childs, G. L. Goodman, and L. S. Goodman, J. Mol. Spectrosc. **86**, 365 (1981).
[9] N. Honjou, G. F. Adams, and D. R. Yarkony, J. Chem. Phys. **79**, 4376 (1983).
[10] (a) J. Nakagawa, P. J. Domaille, T. C. Steimle, and D. O. Harris, J. Mol. Spectrosc. **70**, 374 (1978); (b) M. Dulick, P. F. Bernath, and R. W. Field, Can. J. Phys. **58**, 703 (1980); (c) L. E. Berg, L. Klynning, and H. Martin, Phys. Scr. **21**, 173 (1980); (d) **22**, 216 (1980); (e) P. F. Bernath, R. W. Field, B. Pinchemel, Y. Lefebvre, and J. Schamps, J. Mol. Spectrosc. **88**, 175 (1981); (f) D. E. Reisner, P. F. Bernath, and R. W. Field, J. Mol. Spectrosc. **89**, 107 (1981); (g) L. Klynning and H. Martin, Phys. Scr. **24**, 25 (1981); (h) P. F. Bernath, Ph.D. thesis, Massachusetts Institute of Technology, 1981; (i) P. F. Bernath, P. G. Cummins, and R. W. Field, Chem. Phys. Lett. **70**, 618 (1980); (j) W. J. Childs, G. L. Goodman, and L. S. Goodman, J. Mol. Spectrosc. **86**, 365 (1981); (k) W. E. Ernst and T. Törring, Phys. Rev. A **27**, 875 (1983); (l) W. J. Childs, D. R. Cok, L. S. Goodman, and O. Poulsen, Phys. Rev. Lett. **47**, 1389 (1981); (m) W. J. Childs, D. R. Cok, G. L. Goodman, and L. S. Goodman, J. Chem. Phys. **75**, 501 (1981); (n) W. J. Childs, D. R. Cok, and L. S. Goodman, Can. J. Phys. **59**, 1308 (1981); (o) W. J. Childs, D. R. Cok, and L. S. Goodman, J. Opt. Soc. Am. **72**, 717 (1982).
[11] P. J. Dagdigian, Chem. Phys. Lett. **88**, 225 (1982).
[12] W. E. Ernst, S. Kindt, and T. Törring, Phys. Rev. Lett. **51**, 979 (1983).
[13] S. Kindt, W. E. Ernst, and T. Törring, Chem. Phys. Lett. **103**, 241 (1983).
[14] W. J. Childs, L. S. Goodman, U. Nielsen, and V. Pfeufer, J. Chem. Phys. **80**, 2283 (1984).
[15] G. Herzberg, *Spectra of Diatomic Molecules* (Van Nostrand, New York, 1950), p. 374.
[16] D. L. Hildenbrand, J. Electrochem. Soc. **126**, 1396 (1979).
[17] C. E. Moore, *Atomic Energy Levels*, NSRDS Natl. Bur. Stand. No. 35 (U.S.GPO, Washington, D.C., 1971).
[18] J. C. Slater, Phys. Rev. **36**, 57 (1930).
[19] G. Burns, J. Chem. Phys. **41**, 1521 (1964).
[20] A. W. Weiss, J. Res. Natl. Bur. Stand. Sect. A **71**, 157 (1967).
[21] The locations of the maximum of the function $rR_{nl}(r)$ for $4s$ and $4p$ agree within 1% and for $3d$ within 3% for these two calculations. Small changes such as these will not significantly affect the ligand field matrix elements.
[22] A. S. Douglas and R. H. Garstang, Proc. Cambridge Philos. Soc. **58**, 377 (1962).
[23] W. L. Weise, M. W. Smith, and B. M. Miles, *Atomic Transition Probabilities*, NSRDS Natl. Bur. Stand. No. 22 (U.S.GPO, Washington, D.C., 1969).
[24] L. Pauling, Proc. R. Soc. London Ser. A **114**, 181 (1927).
[25] K. P. Huber and G. Herzberg, *Constants of Diatomic Molecules* (Van Nostrand, New York, 1979), pp. 116–125.
[26] J. L. Dunham, Phys. Rev. **41**, 721 (1932).
[27] H. Hotop and W. C. Lineberger, J. Phys. Chem. Ref. Data **4**, 539 (1975).
[28] D. L. Hildenbrand (private communication).
[29] (a) D. L. Hildenbrand, J. Chem. Phys. **52**, 5751 (1970); (b) **66**, 3526 (1977); (c) P. D. Kleinschmidt and D. L. Hildenbrand, *ibid.* **68**, 2819 (1978).
[30] Λ doubling in $^2\Pi_{3/2}$ arises primarily from the $BJ^{\pm}L^{\mp}$ L-uncoupling operator as expressed in the $q\Lambda$-doubling parameter. The $^2\Pi_{1/2}$ Λ doubling owes primarily to the p parameter which results from a cross term between spin-orbit and L-uncoupling operators and is more difficult to evaluate accurately.
[31] R. N. Zare, A. L. Schmeltekopf, W. J. Harrop, and D. L. Albritton, J. Mol. Spectrosc. **46**, 37 (1973).
[32] J. A. Hall, J. Schamps, J. M. Robbe, and H. Lefebvre-Brion, J. Chem. Phys. **59**, 3271 (1973).

[33]E. A. Colbourn and R. D. Wayne, Mol. Phys. **37**, 1755 (1979).
[34]A. R. Edmonds, *Angular Momentum in Quantum Mechanics*, 2nd ed. (Princeton University, Princeton, N.J., 1960), p. 79.
[35]P. Brumer and M. Karplus, J. Chem. Phys. **58**, 3903 (1973).
[36]A. Dalgarno, Adv. Phys. **11**, 281 (1962).
[37]H. Martin and P. Royer, Chem. Phys. Lett. **97**, 127 (1983).
[38]C. L. Chalek and J. L. Gole, J. Chem. Phys. **65**, 2845 (1976).
[39]D. W. Green, J. Mol. Spectrosc. **40**, 501 (1971).
[40]M. Dulick, Ph.D. thesis, Massachusetts Institute of Technology, 1983.
[41]R. W. Field, Ber. Bunsenges. Phys. Chem. **86**, 771 (1982).
[42]A. Khadjavi, A. Lurio, and W. Happer, Phys. Rev. **167**, 128 (1968).
[43]C. W. Allen, *Astrophysical Quantities* (London University, London, 1963), pp. 66 and 67.